complexes, the reduced quenching ability may be associated with a lower transmission coefficient for energy transfer. In our study the sharp decline in $k_q$ is in accordance with this interpretation, and this is reflected by the value of $k_q = 1.6 \times 10^8$ $M^{-1}$ $s^{-1}$ for the *p*-terphenyl quencher as the $E_T{}^A$ energy of 20600 $cm^{-1}$ is close to the estimated $E_T{}^D$ energy of 20300 (±400) $cm^{-1}$.

The sharp drop of $k_q$ in this region can also be rationalized by consideration of eq 9, as detailed by Balzani and his co-workers,[6]

$$k_q = \frac{k_d}{1 + e^{\Delta G/RT} + \dfrac{k_{-d}}{k_{en}{}^{\circ}}(e^{\Delta G^{*}/RT})} \qquad (9)$$

where $\Delta G^*$ and $\Delta G$ are the free energy of activation and the standard free energy change of the forward energy-transfer step, respectively, $k_d$ is the diffusion-controlled rate constant, and $k_{en}$ is the transmission coefficient. This expression provides a unified view of the so-called "vertical and nonvertical" energy-transfer behavior. It gives a better explanation or understanding for the slight lowering of $k_q$ values of the energy-transfer processes in the endo- or exoergonic regions. The low values of $k_q$ exhibited in this region cannot be attributed to an activation energy term because no such energy is anticipated for isoergonic energy transfer between excited states. Furthermore, low values of the preexponential factor ($k_{en}{}^{\circ}$) arising from "poor" overlap between the donor and acceptor orbitals may lead to reduced $k_q$ values. The $k_{en}{}^{\circ}$ is a function of the electronic interaction energy between initial and final states, which has the form of an exchange integral between donor and acceptor orbitals. As stated above, the exchange energy transfer requires favorable and simultaneous overlap of two orbital pairs in the donor–acceptor couple. Therefore, in our case the reduction in orbital interaction must arise from steric factors and/or the Franck–Condon distortion effects noted above.

**C–D Plateau, Where $E_T{}^D < E_T{}^A$.** In this region quenching is only observed at high [Q]. The energy-transfer processes are expected to be inefficient in this region (even if they are spin-allowed) because there is no overlap of the absorption spectra and, thus, no energy matching. Hence, in theory energy transfer should not take place because the overlap integral of the common electronic states is zero.

The presence of the lower plateau indicates that if energy transfer is occurring, it does not proceed by a simple collisional mechanism from the $^3$MLCT excited state, as eq 9 predicts an exponential decrease in $k_q$ as the energy gap between the donor and acceptor is increased. Considering a coulombic or efficient Forster-type mechanism, it has been shown previously that the rate of energy transfer is also decreased exponentially as the process becomes endothermic according to eq 10,[18e,20] where $\Delta E_T$

$$k_q = k_d \exp(-\Delta E_T/RT) \qquad (10)$$

is a measure of the energy difference between the donor and the acceptor and $k_d$ is the diffusion-controlled rate constant. With use of the obtained $k_d = 3.7 \times 10^9$ $M^{-1}$ $s^{-1}$ and $E_T{}^D = 20300$ $cm^{-1}$ values and the endothermic mechanism (eq 10), the calculated $k_q$ values are for naphthalene $k_q = 2.3 \times 10^7$ $M^{-1}$ $s^{-1}$, benzophenone $k_q = 3.7$ $M^{-1}$ $s^{-1}$, acetophenone $k_q = 1.2 \times 10^{-3}$ $M^{-1}$ $s^{-1}$, and acetone $k_q = 9.2 \times 10^{-6}$ $M^{-1}$ $s^{-1}$, clearly not consistent with our experimental data.

At the present time no convincing rationale has emerged that provides support for an energy-transfer mechanism in the C–D plateau region. Previously, however, the photophysical properties of $(OC)_5W(bpy)W(CO)_5$ have been shown to be solvent sensitive, whereby emission quantum yields and emission lifetimes are diminished as the solution environment becomes more polar; these effects are predominantly manifested in $k_{nr}$ from the $^3$MLCT excited state.[17b] Consequently, it is suggested that the lifetime reductions in the C–D plateau region are associated not with energy transfer but with solvation changes; on addition of these ketones to 0.2–0.5 M the solutions have become quite polar. Another possibility is that under these exceptional conditions of high quencher concentration impurity quenching may take place. However, this possibility is not supported by the fact that the lifetimes were not found to vary following different purification methods of the ketone quenchers.

## Conclusions

Studies of the emission and emission quenching of $(OC)_5W(bpy)W(CO)_5$ have elucidated the nature of energy transfer from the lowest energy excited states in this ligand-bridged organometallic molecule. The $(OC)_5W(bpy)W(CO)_5$ emission is attributed to two close-lying $W(d\pi) \rightarrow \pi^*(bpy)$ metal-to-ligand charge-transfer (MLCT) excited states centered at 20300 (±400) $cm^{-1}$ that are in thermal equilibrium. Both the photophysical decay parameters and the quenching behavior of this complex are consistent with the MLCT states being primarily of triplet character.

Emission lifetime quenching by a range of organic triplet states reveals that several types of energy-transfer mechanisms can take place. When $E_T{}^D$ is at substantially greater energy than $E_T{}^A$, exothermic exchange processes prevail and the observed bimolecular quenching constant approaches the diffusion-controlled limit. As $E_T{}^A$ approaches (or lies narrowly above) $E_T{}^D$, then reversible energy-transfer mechanisms become influential and the quenching efficiency is greatly diminished. When $E_T{}^A$ lies further above $E_T{}^D$, the lifetime reductions are only observed at high quencher concentrations, and they cannot be rationalized with a simple collisional mechanism involving the quencher molecules.

**Acknowledgment.** We are grateful to the donors of the Petroleum Research Fund, administered by the American Chemical Society, for support of this research. M.M.Z. acknowledges receipt of a South African CSIR Fellowship.

**Registry No.** $(OC)_5W(bpy)W(CO)_5$, 81178-10-1; anthracene, 120-12-7; pyrene, 129-00-0; biacetyl, 431-03-8; *p*-terphenyl, 92-94-4; naphthalene, 91-20-3; benzophenone, 119-61-9; acetophenone, 98-86-2; acetone, 67-64-1.

---

(20) Lamola, A. A. In *Energy Transfer and Organic Photochemistry*; Leermakers, P. A., Weissberger, A., Eds.; Techniques of Organic Chemistry, Vol. 14; Wiley: New York, 1969; Chapter 2.

---

Contribution from the Coordination Chemistry Institute,
Nanjing University, Nanjing, P. R. China,
and Chengdu Center of Analysis and Determination,
Academia Sinica, Chengdu, P. R. China

# Crystal Structure and Magnetic Properties of a Novel Hetero Tetranuclear ZnCuCuZn Complex

Yan Zang,*[†] Zhanfeng Yin,[†] Guoxiong Wang,[†] Cheng Zeng,[†] Anbang Dai,[†] and Zhongyuan Zhou[‡]

*Received February 16, 1989*

In recent years, there has been great interest in the magnetic properties of the polynuclear transition-metal complexes, especially the polynuclear copper complexes. Much attention has been focused on the magnetostructural correlations and the exchange mechanism, and a large amount of work has been done and reported.[1] However, most study has been on the chloro-, bromo-, sulfido-, and hydroxo-bridged copper complexes, and much less study exists on the structures and magnetic properties of O–R (where R is aromatic ring) bridged parallel-planar copper complexes and none on the correlation between the magnetic and structural characteristics of these complexes.

Recently, we have determined the crystal structure and magnetic properties of binuclear copper complex with picolinaldehyde *N*-oxide thiosemicarbazone.[2] This compound shows a parallel-planar structure, in which two copper(II) ions are linked by the

---

[†] Nanjing University.
[‡] Academia Sinica.

**Table I.** Crystallographic Data for $(CuLZnCl_4)_2$

| | |
|---|---|
| formula | $C_{28}H_{28}Cl_8Cu_2N_8O_4Zn_2$ |
| fw | 1082.0 |
| space group | $C_{2h}^5$-$P2_1/n$ (No. 14) |
| *a*, Å | 8.965 (6) |
| *b*, Å | 20.336 (8) |
| *c*, Å | 10.649 (5) |
| $\beta$, deg | 95.20 (4) |
| *V*, $Å^3$ | 1933.32 (1.2) |
| *Z* | 2 |
| *T*, °C | 22 |
| $\lambda$(Cu K$\alpha$), Å | 1.541 78 |
| $\rho_{calcd}$, g $cm^{-3}$ | 1.85 |
| $\mu$, $cm^{-1}$ | 82.86 |
| transm coeff | 0.942–0.782 |
| total no. of reflcns collcd | 2521 |
| no. of reflcns with $I \geqslant 3\sigma(I)$ | 2037 |
| $R(F_o)$ | 0.0681 |
| $R_w(F_o)$ | 0.0707 |

two oxygen atoms of the *N*-oxide, and exhibits antiferromagnetic coupling with $2J = -34$ $cm^{-1}$. Here we report the results of the synthesis, structure, and magnetic properties of a novel hetero tetranuclear ZnCuCuZn complex.

## Experimental Section

**Synthesis.** Picolinaldehyde *N*-oxide was prepared according to the reference method.[3]

$[CuL(H_2O)](ClO_4)_2$ (L = 2,2'-[1,2-Ethanediylbis(nitrilomethylidyne)]bis(pyridine *N*-oxide)). Picolinaldehyde *N*-oxide (0.98 g) was dissolved in dilute ethanol and heated; then, ethylenediamine (0.24 g) was added with stirring. After 15 min, a solution of $Cu(ClO_4)_2 \cdot 6H_2O$ (1.47 g) was mixed with it, and then the solvent was slowly evaporated till dark violet crystals formed. The product was separated by filtration, washed with ethanol, and finally vacuum-dried. Anal. Calcd for $C_{14}H_{16}Cl_2CuN_4O_{11}$: Cu, 11.54; C, 30.33; H, 2.93; N, 10.17. Found: Cu, 11.19; C, 30.09; H, 2.78; N, 10.40.

**$(CuLZnCl_4)_2$.** $ZnCl_2$ (0.5 g) was dissolved in 50 mL of methanol and then added to the acetonitrile solution (50 mL) of $[CuL(H_2O)](ClO_4)_2$ (0.5 g). Upon slow evaporation, dark crystals formed. The product was filtered, washed with methanol and ancetonitrile, and dried. Anal. Calcd for $C_{28}H_{28}Cl_8Cu_2N_8O_4Zn_2$: Cu, 11.74; Zn, 12.09; C, 31.06; H, 2.59; N, 10.35. Found: Cu, 11.71; Zn, 12.16; C, 31.11; H, 2.61; N, 9.91.

**X-ray Data Collection.** A dark crystal of the tetranuclear complex, with dimensions of 0.40 × 0.44 × 0.60 $mm^3$, was mounted on Nicolet-R3M/E four-cyclic diffractometer equipped with graphite-monochromatized Cu K$\alpha$ radiation. The crystal is monoclinic. The cell dimensions were determined by a least-squares refinement of setting angles of 25 reflections. The intensity data were collected at room temperature by the $\theta$–$2\theta$ scan technique in the scan range $3° \leq 2\theta \leq 105°$. The intensities and their standard deviations were corrected for Lorentz-polarization effects. A total of 2521 independent reflections were processed, in which 2037 had $I \geqslant 3\sigma(I)$. Only these latter data were used in the refinement. Pertinent experimental conditions and crystallographic data are summarized in Table I.

**Solution and Refinement of the Structure.** The positions of zinc, copper, and chlorine atoms were determined from a three-dimensional Patterson synthesis. The other non-hydrogen atoms were located in a subsequent difference Fourier synthesis. Refinement was carried out with the use of anisotropic thermal parameter for all the non-hydrogen atoms. The contribution of hydrogen atoms at their calculated positions, with C–H = 0.96 Å and overall isotropic thermal parameter $U = 0.04$ $Å^2$, was included. The final $R = \sum|F_o - |F_c||/\sum F_o$ was 0.0681 ($R_w = \sum w|F_o - |F_c||/\sum wF_o$ was 0.0707; $w = 1/[(\sigma^2(F_o) + |g|(F_o)^2)]$).

**Magnetic Susceptibility Measurements.** Magnetic susceptibility data were collected on a powder sample by use of a CF-1 extracting-sample magnetometer installed at the Institute of Physics, Acadimia Sinica, Beijing, China. The data were corrected to compensate for the diamagnetism of the constituent atoms and for the temperature-independent paramagnetism of the Cu(II) ions ($60 \times 10^{-6}$ cgsu).[4,5]

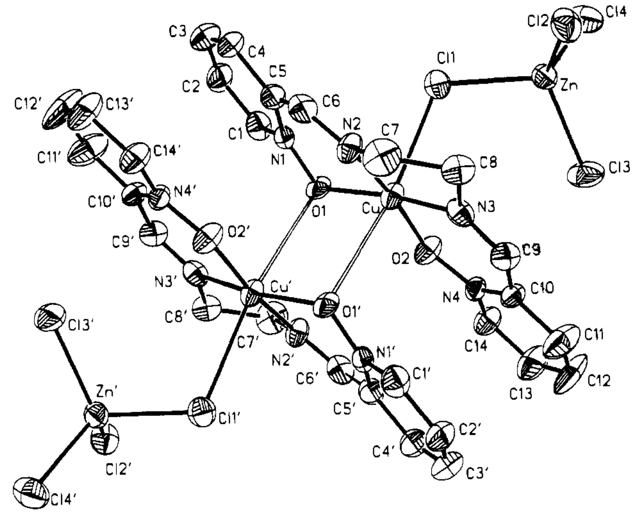

Figure 1. Tetrameric molecular structure (hydrogen atoms are omitted).

**Table II.** Atomic Coordinates ($\times 10^4$) and Isotropic Thermal Parameters ($Å^2 \times 10^3$)

| | *x* | *y* | *z* | $U^a$ |
|---|---|---|---|---|
| Zn | 5507 (1) | 3475 (1) | 1807 (1) | 32 (1) |
| Cu | 8734 (1) | 4464 (1) | 4083 (1) | 28 (1) |
| Cl(1) | 7022 (2) | 4387 (1) | 1836 (2) | 38 (1) |
| Cl(2) | 6922 (2) | 2646 (1) | 1138 (2) | 44 (1) |
| Cl(3) | 4780 (2) | 3300 (1) | 3738 (2) | 57 (1) |
| Cl(4) | 3395 (2) | 3595 (1) | 503 (2) | 51 (1) |
| O(1) | 9143 (5) | 5385 (2) | 3817 (4) | 31 (2) |
| N(1) | 9662 (6) | 5601 (3) | 2763 (6) | 30 (2) |
| C(1) | 9254 (8) | 6218 (4) | 2403 (7) | 37 (3) |
| C(2) | 9810 (9) | 6511 (4) | 1380 (8) | 45 (3) |
| C(3) | 10779 (10) | 6158 (4) | 698 (8) | 54 (3) |
| C(4) | 11168 (9) | 5542 (4) | 1035 (7) | 46 (3) |
| C(5) | 10605 (8) | 5243 (4) | 2073 (7) | 35 (3) |
| C(6) | 11074 (8) | 4576 (4) | 2448 (7) | 36 (3) |
| N(2) | 10481 (6) | 4232 (3) | 3227 (6) | 33 (2) |
| C(7) | 11001 (8) | 3563 (4) | 3516 (9) | 45 (3) |
| C(8) | 9654 (8) | 3148 (4) | 3773 (7) | 35 (2) |
| N(3) | 8714 (6) | 3548 (3) | 4508 (6) | 31 (2) |
| C(9) | 8004 (8) | 3287 (4) | 5357 (7) | 33 (2) |
| C(10) | 6986 (8) | 3625 (3) | 6124 (7) | 29 (2) |
| C(11) | 6349 (11) | 3269 (4) | 7046 (8) | 58 (3) |
| C(12) | 5326 (12) | 3555 (4) | 7748 (10) | 68 (4) |
| C(13) | 4957 (10) | 4196 (4) | 7564 (9) | 54 (3) |
| C(14) | 5605 (8) | 4547 (4) | 6666 (7) | 38 (3) |
| N(4) | 6623 (6) | 4274 (3) | 5978 (5) | 27 (2) |
| O(2) | 7205 (5) | 4673 (2) | 5159 (5) | 35 (2) |

[a] Equivalent isotropic *U* defined as one-third of the trace of the orthogonalized $U_{ij}$ tensor.

**EPR Spectra.** EPR spectra were recorded on a JEOL-FEIXG EPR spectrometer operating at the X-band (9.177 GHz) frequency.

## Results and Discussion

**Structural Information.** The complex is a tetranuclear molecule, shown in Figure 1. Final position parameters, bond lengths, and bond angles are given in Tables II and III.

In each molecule, the ligand environments of the copper atoms are identical owing to the crystallographic inversion symmetry. Each copper atom shows distorted 4 + 1 + 1 square-bipyramidal coordination. The four short bonds are to the two nitrogens, N(2) and N(3), and two oxygens, O(1) and O(2), of the tetradentate bis(Schiff base) ligand. The N(2), N(3), O(1), O(2), and Cu atoms lie approximately in a plane; the maximum deviation from planarity is 0.12 Å (Cu). The copper atom of the approximately planar fragment is linked via a weak fifth bond to the in-plane-

---

(1) For reviews see: (a) Hatfield, W. E. In *Magneto-structural Correlations in Exchange Coupled Systems*; Reidel: Dordrecht, The Netherlands, 1985; p 555. (b) Willett, R. D. *Ibid.*; p 389. (c) Hodgson, D. J. *Prog. Inorg. Chem.* **1975**, *19*, 173. (d) Hatfield, W. E. *Comments Inorg. Chem.* **1981**, *1*, 105 and references therein. (e) Melnic, M. *Coord. Chem. Rev.* **1982**, *42*, 259.

(2) Zang, Yan; Wang, Guoxiong; Zeng, Cheng; Dai, Anbang. *Kexue Tongbao*, in press.

(3) Jerchel, D.; Heider, J.; Wagner, H. *Justus Liebigs Ann. Chem.* **1958**, *613*, 155.

(4) Earnshaw, A. *Introduction to Magnetochemistry*; Academic Press: London, 1968.

(5) For example, see: Towle, D. K.; Hoffmann, S. K.; Hatfield, W. E.; Singh, P.; Chaudhuri, P.; Wieghardt, K. *Inorg. Chem.* **1985**, *24*, 4393.

**Table III.** Bond Lengths (Å) and Bond Angles (deg)

(a) Bond Lengths

| | | | |
|---|---|---|---|
| Zn-Cl(1) | 2.297 (2) | Zn-Cl(2) | 2.264 (2) |
| Zn-Cl(3) | 2.241 (2) | Zn-Cl(4) | 2.257 (2) |
| Cu-Cl(1) | 2.727 (2) | Cu-O(1) | 1.934 (4) |
| Cu-N(2) | 1.941 (6) | Cu-N(3) | 1.917 (5) |
| Cu-O(2) | 1.913 (5) | O(1)-N(1) | 1.329 (8) |
| C(5)-C(6) | 1.464 (11) | O(6)-N(2) | 1.241 (10) |
| N(2)-C(7) | 1.462 (9) | C(7)-C(8) | 1.519 (10) |
| C(8)-N(3) | 1.452 (9) | N(3)-C(9) | 1.269 (10) |
| C(9)-C(10) | 1.453 (10) | N(4)-O(2) | 1.332 (7) |
| O(1)-Cu′ | 2.819 | | |

(b) Bond Angles

| | | | |
|---|---|---|---|
| Cl(1)-Zn-Cl(2) | 105.0 (1) | Cl(1)-Zn-Cl(3) | 109.7 (1) |
| Cl(2)-Zn-Cl(3) | 112.8 (1) | Cl(1)-Zn-Cl(4) | 112.5 (1) |
| Cl(2)-Zn-Cl(4) | 110.5 (1) | Cl(3)-Zn-Cl(4) | 106.5 (1) |
| Cl(1)-Cu-O(1) | 91.5 (1) | Cl(1)-Cu-N(2) | 89.3 (2) |
| O(1)-Cu-N(2) | 89.7 (2) | Cl(1)-Cu-N(3) | 97.7 (2) |
| O(1)-Cu-N(3) | 168.9 (2) | N(2)-Cu-N(3) | 84.3 (3) |
| Cl(1)-Cu-O(2) | 99.3 (1) | O(1)-Cu-O(2) | 91.6 (2) |
| N(2)-Cu-O(2) | 171.2 (2) | N(3)-Cu-O(2) | 93.0 (2) |
| Zn-Cl(1)-Cu | 110.1 (1) | Cu-O(1)-N(1) | 122.0 (4) |
| N(1)-C(5)-C(6) | 121.3 (7) | O(1)-N(1)-C(5) | 123.7 (6) |
| C(5)-C(6)-N(2) | 125.1 (7) | Cu-N(2)-C(6) | 126.1 (5) |
| Cu-N(2)-C(7) | 112.5 (5) | C(6)-N(2)-C(7) | 121.2 (7) |
| N(2)-C(7)-C(8) | 108.2 (6) | C(7)-C(8)-N(3) | 107.2 (6) |
| Cu-N(3)-C(8) | 113.5 (5) | Cu-N(3)-C(9) | 126.3 (5) |
| C(8)-N(3)-C(9) | 120.1 (6) | N(3)-C(9)-C(10) | 125.7 (7) |
| Cu-O(2)-N(4) | 126.9 (4) | O(1)-Cu-O(1′) | 83.6 |
| Cu-O(1)-Cu′ | 96.4 | C(9)-C(10)-N(4) | 123.3 (6) |
| | | C(10)-N(4)-O(2) | 124.1 (6) |

coordinated oxygen atom, O(1′), of the other. Therefore, each bridging oxygen atom simultaneously occupies an in-plane coordination site of one cooper (II) ion and an apical site of the other. The long out-of-plane bond distance is longer than most of those reported for structures involving parallel-planar units linked by relative long out-of-plane bonds, but is slightly shorter than that in β-bis(8-hydroxyquinolinato)Copper.[6] The four-membered $Cu_2O_2$ bridging unit is strictly planar owing to the inversion symmetry. There is a sixth bond between chlorine, Cl(1), and Cu to form the square-bipyramidal configuration. Cl(1) is simultaneously coordinated to Cu(II) and Zn(II). The ligand environments of zinc atoms are also identical because of the inversion symmetry. Each Zn atom shows a tetrahedral coordination, only a small distortion being found. The chlorine atoms occupy the four coordination sites. Between Cu(II) and Zn(II), there is a single bridging chlorine atom; such singly bridged species are less common than doubly bridged systems.[1a,7] The bond lengths in the bis(Schiff base) ligand have their usual values within error limits. It should be emphasized that in each bis(Schiff base) ligand, the planes of the pyridine *N*-oxides are not coplanar with the copper coordination base plane as in the salen complexes,[15] forming dihedral angles of 22 and 14°, respectively.

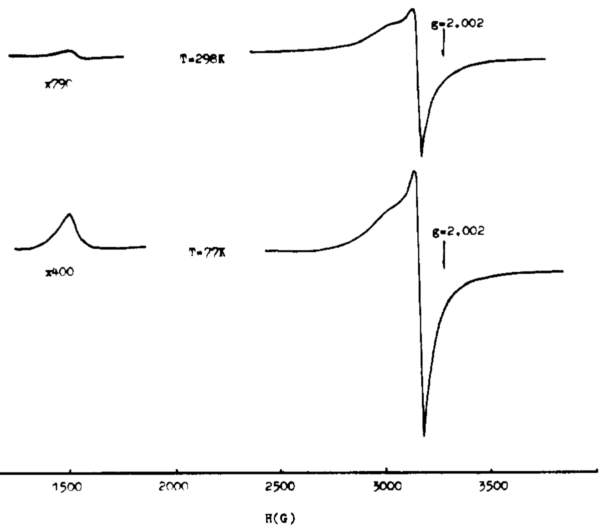

**Figure 2.** EPR X-band powder spectra of $(CuLZnCl_4)_2$.

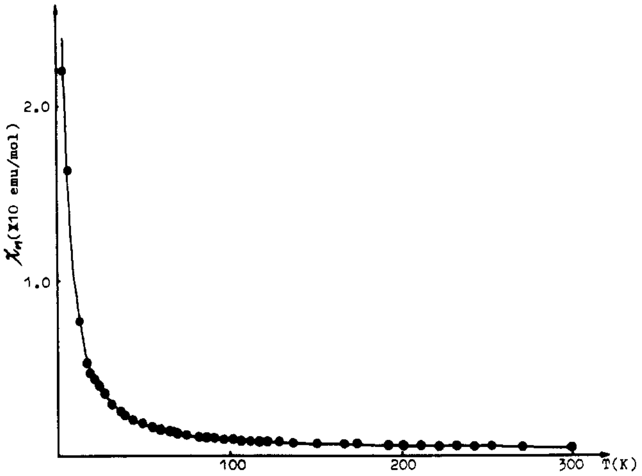

**Figure 3.** Magnetic susceptibility data for $(CuLZnCl_4)_2$. The solid line through the data was generated by eq 2 with $J = 4.6$ cm$^{-1}$, $ZJ' = 0.4$ cm$^{-1}$.

**Magnetic Properties.** EPR spectra of polycrystalline material were recorded at X-band frequency and at both room-temperature and (down to) 77 K. The spectra show a transition at $\langle g \rangle = 2.10$ with apparent values of $g_\perp = 2.06$ and $g_\parallel = 2.16$ (7). In addition, a low-field resonance corresponding to the $\Delta M_s = 2$ transition was observed. This transition is characteristic of a magnetically coupled dimeric copper center and is in agreement with the crystal structure. Spectra recorded at room temperature and 77 K are given in Figure 2. The intensity of the spectrum increases as the temperature lowers from room temperature to 77 K. The overall increase in intensity and especially the increase in low-field transition is consistent with the existence of ferromagnetically coupled dimeric center. The observation of a $\Delta M_s = 2$ line indicates that the intermolecular coupling is not significant as compared with the intramolecular exchange interaction.

Magnetic susceptibility data have been collected from 4.2 to 300 K. The molar magnetic susceptibility of the complex is plotted as a function of temperature in Figure 3. The exchange-interaction Hamiltonian is of the form $-2J\hat{S}_1{\cdot}\hat{S}_2$ from which we have defined $-2J = \Delta E_{ST}$ for pairs of $S = {}^1/_2$ ions. The magnetic expression[8] is

$$\chi = \frac{Ng^2\beta^2}{kT}\,\frac{1}{3 + \exp(-2J/kT)} \tag{1}$$

with molecular field correction[5]

$$\chi' = \frac{\chi}{1 - (2ZJ'/Ng^2\beta^2)\chi} \tag{2}$$

where $Z$ is the number of the nearest-neighbor molecules and $J'$

---

(6) Inman, G. W.; Hatfield, W. E.; Drake, R. F. *Inorg. Chem.* **1972**, *11*, 2425.

(7) Marsh, W. E.; Hatfield, W. E.; Hodgson, D. J. *Inorg. Chem.* **1982**, *21*, 2679 and references therein.

(8) Bleaney, B.; Bowers, K. D. *Proc. R. Soc. London* **1952**, *A214*, 451.

(9) Kahn, O. In *Magneto-structural Correlations in Exchange Coupled Systems*; Reidel: Dordrecht, The Netherlands, 1985; p 39.

(10) Crawford, W. H.; Richardson, H. W.; Wasson, J. R.; Hodgson, D. J.; Hatfield, W. E. *Inorg. Chem.* **1976**, *15*, 2107.

(11) Roundhill, S. G. N.; Roundhill, D. M.; Bloomquist, D. R.; Landee, C.; Wellett, R. D.; Dooley, D. M.; Gray, H. B. *Inorg. Chem.* **1979**, *18*, 831.

(12) Hatfield, W. E. *Inorg. Chem.* **1983**, *22*, 837.

(13) Marsh, W. E.; Bowman, T. L.; Harris, C. S.; Hatfield, W. E.; Hodgson, D. J. *Inorg. Chem.* **1981**, *20*, 3864 and references therein.

(14) Chiari, B.; Helms, J. H.; Piovesana, O.; Tarantelli, T.; Zanazzi, P. F. *Inorg. Chem.* **1986**, *25*, 2408.

(15) (a) Hall, D.; Waters, T. N. *J. Chem. Soc.* **1960**, 2644. (b) Simpson, G. D.; Carlisle, G. O.; Hatfield, W. E. *J. Inorg. Nucl. Chem.* **1974**, *36*, 2257.

(16) (a) Hatfield, W. E. *Inorg. Chem.* **1972**, *11*, 216. (b) Hall, D.; Sheat, S. V.; Waters, T. N. *J. Chem. Soc. A* **1968**, 460.

(17) (a) Hatfield, W. E.; Barnes, J. A.; Jeter, D. Y.; Whyman, R.; Jones, E. R. *J. Am. Chem. Soc.* **1970**, *92*, 4982. (b) McGregor, K. T.; Barnes, J. A.; Hatfield, W. E. *J. Am. Chem. Soc.* **1973**, *95*, 7993.

**Table IV.** Structural and Magnetic Data for Parallel-Planar Copper Complexes[a]

| compd | $2J$, $cm^{-1}$ | $\phi$, deg | $R$, Å | $\phi/R$, deg/Å | ref |
|---|---|---|---|---|---|
| $[Cu(Salen)]_2$ (**1**) | 18 | 89 | 2.4 | 37.1 | 15 |
| $[Cu(CH_3Sal)_2]_2$ (**2**) | 8 | 100 | 2.45 | 40.9 | 16 |
| $[Cu(8\text{-}Oquin)_2]_2$ (**3**) | −1 | 90.5 | 2.83 | 32.0 | 6 |
| $[Cu(pyO)_2(NO_3)_2]_2$ (**4**) | 10 | 102.9 | 2.44 | 42.2 | 17 |
| $[Cu(4\text{-}CH_3pyO)_2(NO_3)_2]_2$ (**5**) | 2 | 101.8 | 2.58 | 39.4 | 1e, 17b |
| $[Cu(piotsc)(H_2O)]_2(NO_3)_2$ (**6**) | −34 | 97.8 | 2.68 | 36.5 | 2 |
| $(CuLZnCl_4)_2$ (**7**) | 9.3 | 96.4 | 2.82 | 34.2 | *b* |

[a] Key: Salen = *N*,*N*′-ethylenebis(salicylaldiminate) ion; $CH_3sal$ = *N*-methylsalicylaldiminate ion; 8-Oquin = 8-hydroxyquinolate ion; pyO = pyridine *N*-oxide; 4-$CH_3pyO$ = 4-methylpyridine *N*-oxide; piotsc = picolinaldehyde *N*-oxide thiosemicarbazone; L = 2,2′-[1,2-ethanediylbis(nitrilomethylidyne)]bis(pyridine *N*-oxide). [b] This work.

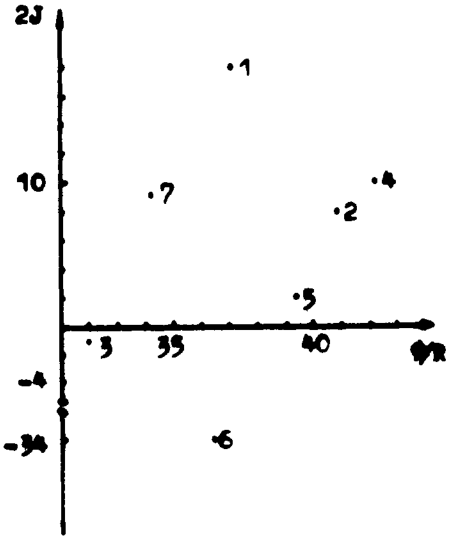

**Figure 4.** $2J$ and $\phi/R$ data for some bis(O–R) (R is aromatic ring) bridged parallel-planar copper complexes.

is the lattice-interaction parameter. This equation was used to fit the experimental data, and we found that $g = 2.09$, $J = 4.6$ $cm^{-1}$, and $ZJ' = -0.4$ $cm^{-1}$. The best fit is indicated by the solid line in Figure 3 and represents a good description of the experimental data. One may note that the $g$ values obtained from both the best fit of the magnetic susceptibility and the EPR experiment are in good agreement with each other. The existence of weakly ferromagnetic coupling between the Cu atoms in the tetranuclear complex is also supported by the EPR spectra.

In order to understand the mechanism of exchange in the complex, we have examined the magnetic orbitals by CNDO/2 calculations. The magnetic orbital[9] obtained by calculating on a half-molecular fragment containing one Cu and one Zn and their surrounding atoms is of the form

$$\psi_A = 0.58d_{x^2-y^2}(Cu) - 0.314p_z(O(1)) + 0.505p_x(O(1')) + 0.557p_z(O(1'))$$

The other magnetic orbital, $\psi_B$, has the same form owing to the inversion symmetry. It is clear that there is no antiferromagnetic exchange interaction in the complex because the overlap integral between magnetic orbitals is zero.

Magnetostructural correlations for copper complexes have been studied by many researchers. It has been found that for both hydroxo-[10] and chloro-bridged[11] planar copper dimers, plotting of $J$ versus bridging angle $\phi$ gives a straight line. For the parallel-planar copper complexes, it was suggested that the $2J$ be determined both by the bridging angle $\phi$ and by the out-of-plane bond length $R$.[1a–c,12] The plot of $2J$ versus $\phi/R$ gives a smooth curve or surface. It seems true for chloro- and bromo-bridged copper complexes.[1a–c,13] In one-atom carboxylato-bridged copper complexes, the same trend has been found.[14]

The data for some known bis(O–R) (where R is an aromatic ring) bridged parallel-planar copper complexes that have been magnetically and structurally characterized are given in Table IV. The $2J$ and $\phi/R$ data are shown in Figure 4. The data obviously do not lie on a smooth curve. It is clear that there is no "simple" magnetostructural correlation for such magnetically coupled copper complexes, and further studies should be needed.

**Registry No.** $[CuL(H_2O)](ClO_4)_2$, 121577-91-1; $(CuLZnCl_4)_2$, 124605-59-0; picolinaldehyde *N*-oxide, 7216-40-2; ethylenediamine, 107-15-3.

**Supplementary Material Available:** Tables SI–SIV, listing anisotropic thermal parameters, hydrogen positions and isotropic thermal parameters, bond angles and distances associated with the pyridyl ring, and experimental and calculated magnetic susceptibility data (5 pages); tables of calculated and observed structure factors (12 pages). Ordering information is given on any current masthead page.

---

Contribution from the Laboratoire de Chimie de Coordination
du CNRS,[†] 205 route de Narbonne,
31077 Toulouse Cedex, France

## Reaction of $Li[(CO)_5WPPh_2]$ with $[RhCl(C_8H_{12})]_2$: Unexpected Synthesis of the Linear Trimetallic Complex $(CO)_4W(\mu\text{-}PPh_2)_2Rh(\mu\text{-}CO)_2Rh(C_8H_{12})$

Marine Cazanoue, Françoise Dahan, and René Mathieu*

*Received May 12, 1989*

In pursuing our interest in the synthesis and study of the reactivity of mixed polymetallic complexes containing metals of group 6,[1,2] we have attempted the synthesis of mixed dinuclear group 6–rhodium compounds using the "bridged-assisted" synthetic pathway.[3] The literature gives examples of bimetallic complexes associating tungsten and rhodium through two diphenylphosphido groups,[4] but our aim was to have a bimetallic system bridged with only one diphenylphosphido group to minimize steric crowding around the metallic centers.

For this reason we have checked the reaction of $Li[W(CO)_5PPh_2]$ with 0.5 equiv of $[Rh(\mu\text{-}Cl)(COD)]_2$ expecting the formation of $(CO)_5W(\mu\text{-}PPh_2)Rh(COD)$. In fact the reaction is more complex than expected, and here we report the result of this study.

### Results

$Li[W(CO)_5PPh_2]$ reacts with 0.5 equiv of $[Rh(\mu\text{-}Cl)(COD)]_2$ to give an orange solution. Examination of the crude product of the reaction by $^{31}P$ NMR spectroscopy gives evidence of the formation of two products: one singlet with satellites due to coupling with $^{183}W$ centered at 181 ppm corresponds to one product and a doublet of doublets with $^{183}W$ satellites centered at 177 ppm corresponds to the other.

These results suggest that only one of the products formed contains rhodium metal.

The two products have been separated by column chromatography. Product **1**, the minor component, is a dark red solid that corresponds to the single peak centered at 181 ppm. This information coupled with the compound's infrared spectrum ($\nu_{CO}$($CH_2Cl_2$) 2028, 1925 $cm^{-1}$) is consistent with the published data given for $[W(CO)_4(\mu\text{-}PPh_2)]_2$.[5]

The second product **2** is a brown solid, the analysis of which is consistent with the $WRh_2(CO)_6(PPh_2)_2(C_8H_{12})$ formulation. Its $^{31}P$ NMR spectrum is centered at 177 ppm and shows satellites due to coupling with the $^{183}W$ atom. Two coupling constants with the $^{101}Rh$ nucleus are observed, one with a value of 158 Hz, the other of 4.7 Hz. These data suggest that the phosphorus atoms in **2** are directly bonded to a tungsten and a rhodium atom and that they then have a long range coupling with a second atom of

---

[†] Unité No. 8241 liée par conventions à l'Université Paul Sabatier et à l'Institut National Polytechnique.

0020-1669/90/1329-0563$02.50/0